Chemical, Computational, and Structural Studies of Dimeric (Pentamethylcyclopentadienyl)zirconium Thiolate and Alkoxide Complexes

Richard H. Heyn and Douglas W. Stephan*

Department of Chemistry and Biochemistry, University of Windsor, Windsor, ON, Canada N9B 3P4

Received December 2, 1994[⊗]

The compounds $[Cp^*Zr(SR)_2(\mu_2\text{-}SR)]_2$ (R = Bz (**6**), Et (**7**)) are prepared via reaction of Cp^*ZrCl_3 with 3 equiv of the respective sodium thiolate. The NMR data of **6** are consistent with a symmetric dimer in which two thiolate ligands bridge two Zr centers and the pentamethylcyclopentadienyl ligands adopt a *cisoid* geometry. In the case of **7**, a mixture of three isomers of the dimeric complex is observed (*cisoid* (*syn*) **7a**, *transoid* (*anti*) **7b**, and *transoid* (*syn*) **7c**). These species have been characterized by high-field NMR as well as crystallography in the case of **7b**. Reaction of **6** with PMe_3 results in the monomeric adduct $Cp^*Zr(SBz)_3(PMe_3)$ (**8**). Reaction of **6** with MeOH yields the *transoid* dimer species $[Cp^*Zr(OMe)_2(\mu\text{-}OMe)]_2$ (**9**). The species $[Cp^*Zr(SBz)]_2(\mu_2\text{-}SBz)_3(\mu_3\text{-}O)Li(THF)$ (**10**) is also prepared and structurally characterized. Molecular mechanics and EHMO calculations of models based on the structures of **7b** and **9** infer that the planarity at the bridging S or O atoms in these dimers arises as a result of steric factors rather than π-bonding. This view is supported to some extent by the crystallographic study of **10**. Compound **7b** crystallizes in the space group $P\bar{1}$, with $a = 9.580(3)$ Å, $b = 12.210(2)$ Å, $c = 9.222(3)$ Å, $\alpha = 95.01(2)°$, $\beta = 108.55(2)°$, $\gamma = 72.62(2)°$, $V = 976.0(5)$ Å^3, and $Z = 1$. Compound **9** crystallizes in the space group $P2_1/n$, with $a = 12.540(3)$ Å, $b = 9.694(3)$ Å, $c = 13.165(3)$ Å, $\beta = 107.16(2)°$, $V = 1529.3(7)$ Å^3, and $Z = 2$. Compound **10** crystallizes in the space group $P\bar{1}$, with $a = 12.907(8)$ Å, $b = 22.270(6)$ Å, $c = 11.610(8)$ Å, $\alpha = 99.81(3)°$, $\beta = 114.59(6)°$, $\gamma = 79.24(3)°$, $V = 2965(3)$ Å^3, and $Z = 2$.

Introduction

Thiolate derivatives of the early transition metals, in particular metallocene derivatives, have received considerable attention in recent years.[1] In contrast, comparatively little is known about analogous *mono*cyclopentadienyl species despite the fact that the first report of such a species was in 1968 when Kopf and Block described the preparation of $CpTi(SPh)Cl_2$.[2] Although a few subsequent studies have reported related species,[3−12] it was not until our recent papers that a systematic study of the chemistry of such complexes began. The complexes $CpTi(SCH_2CH_2CH_2S)Cl$ (**1**) and $CpTi(SCH_2CH_2SCH_2CH_2S)Cl$ (**2**)[13] and the dimeric compound $[CpTi(SCH_2CH_2S)Cl]_2$ (**3**)[14] illustrate the variable geometry at Ti as these compounds adopt pseudo-tetrahedral, pseudo-trigonal bipyramidal, and pseudo-square pyramidal (dimeric) coordination spheres, respectively (Chart 1). The related *tri*thiolate species $CpTi(SCH_2CH_2CH_2S)SPh$ (**4**) and $[CpTi(SCH_2CH_2S)(SPh)]_2$ are readily derived from **1** and **2**, respectively, while reaction of **1** with two additional equivalents of NaSPh yields the "*four legged piano stool*" complex $[CpTi(SCH_2CH_2CH_2S)(SPh)_2]Na$.[15] Crystallographic characterization of the related species $[CpTi(SCH_2CH_2CH_2S)_2Na(THF)_x]_n$ ($x = 1$, $x = 2$ (**5**)) revealed that these species form infinite polymeric chain structures in the solid state. The nature of the Lewis acidic metal center in these monocyclopentadienyltitanium thiolates has been examined by both reactivity and theoretical studies.[13] Most recently, we have described the use of **1** in the metal-mediated synthesis of organosulfur derivatives.[16] This success, together with the total absence of related *mono*cyclopentadienylzirconium thiolate derivatives in the literature, has prompted us to initiate a systematic study of related CpZr−thiolate chemistry. In this, our initial report, we describe the synthesis, structure, and bonding of the first CpZr−thiolate derivatives.

Experimental Section

General Data. All preparations were done under an atmosphere of dry, O_2-free N_2 by employing either Schlenk line techniques or a Vacuum Atmospheres inert atmosphere glovebox equipped with a 5 ft^3/min recirculating purifier. Solvents were reagent grade, distilled from the appropriate drying agents under N_2 and degassed by the freeze−thaw method at least three times prior to use. ^1H and ^{13}C spectra were recorded on a Bruker AC-300 operating at 300 and 81 MHz, respectively. $^{31}P\{^1H\}$ NMR spectra were recorded on a Bruker AC-200 operating at 75 MHz. Trace amounts of solvents were used as references, and chemical shifts are reported relative to $SiMe_4$ and 85% H_3PO_4, respectively. Combustion analyses were performed by Schwarzkopf Laboratories, Woodside, NY. Cp^*ZrCl_3 was purchased from the Strem Chemical Co. Some of these samples proved to be $Cp^*ZrCl_3{\cdot}LiCl$.

Synthesis of $[Cp^*Zr(SR)_2(\mu^2\text{-}SR)]_2$ (R = Bz (6), Et (7)). These complexes were prepared in a similar manner, and thus only one

[⊗] Abstract published in *Advance ACS Abstracts,* May 1, 1995.

(1) Stephan, D. W.; Nadasdi, T. T. *Coord. Chem. Rev.* **1995**, in press.
(2) Köpf, H.; Block, B. Z. *Naturforsch.* **1968**, *B23*, 1534.
(3) Coutts, R. S. P.; Wailes, P. C. *J. Organomet. Chem.* **1974**, *73*, C5.
(4) (a) Dormond, A.; Kolavudh, T.; Tirouflet, J. *J. Organomet. Chem.* **1979**, *164*, (1979) 317. (b) Dormond, A.; Kolavudh, T. *J. Organomet. Chem.* **1977**, *125*, 63.
(5) Klapoetke, T.; Laskowski, R.; Köpf, H. *Z. Naturforsch., B: Chem. Sci.* **1987**, *42*, 777.
(6) Klapoetke, T.; Köpf, H.; Gowik, P. *J. Chem. Soc., Dalton Trans.* **1988**, 1529.
(7) (a) Dey, K.; Koner, D.; Biswas, A. K.; Ray, S. *J. Chem. Soc., Dalton Trans.* **1982**, 911. (b) Dey, K.; Ray, S.; Koner, D. *Proc. Indian Acad. Sci.: Chem. Sci.* **1983**, *92*, 257.
(8) Alyea, E. C.; Malek, A. *Inorg. Nucl. Chem. Lett.* **1977**, *13*, 587.
(9) Köpf, H.; Grabowski, S. Z. *Anorg. Allg. Chem.* **1983**, *496*, 167.
(10) Cardin, C. J.; Roy, A. *Inorg. Chim. Acta* **1985**, *107*, L33.
(11) Alyea, E. C.; Malek, A.; Merrell, P. H. *J. Coord. Chem.* **1974**, *4*, 55.
(12) Alyea, E. C.; Malek, A. *Inorg. Nucl. Chem. Lett.* **1977**, *13*, 587.
(13) Nadasdi, T. T.; Huang, Y.; Stephan, D. W. *Inorg. Chem.* **1993**, *32*, 347.
(14) Nadasdi, T. T.; Stephan, D. W. *Inorg. Chem.* **1993**, *32*, 5933.
(15) Nadasdi, T. T.; Stephan, D. W. *Inorg. Chem.* **1994**, *33*, 1532.
(16) Huang, Y.; Nadasdi, T. T.; Stephan, D. W. *J. Am. Chem. Soc.* **1994**, *116*, 5483.

0020-1669/95/1334-2804$09.00/0 © 1995 American Chemical Society

Chart 1

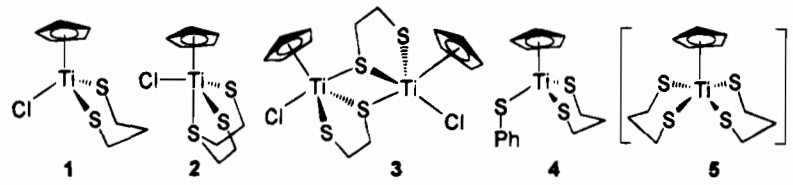

preparation is described. A flask was charged with Cp^*ZrCl_3 (0.26 g, 0.78 mmol) and NaSBz (0.31 g, 2.3 mmol), and benzene (25 mL) was added. The mixture was stirred for 18 h, and the resulting mixture was filtered and washed with benzene (3 × 5 mL). The combined filtrate and washes were evaporated to dryness yielding an oily residue. Addition of hexane (10 mL) followed by filtration provided **6** as a yellow powder in 90% yield. Both **6** and **7** were recrystallized from hexane, although **6** is only sparingly soluble.

6. ^1H NMR (C_6D_6, 25 °C, δ): 1.97 (s, 15 H, C_5CH_3), 4.76 (s, 2 H, μ_2-SCH_2), 4.82 (d, $|^2J_{H-H}|$ = 13.7 Hz, 2 H, SCH_2), 5.11 (d, $|^2J_{H-H}|$ = 13.7 Hz, 2 H, SCH_2), 7.06 (m, 9 H, *m,p*-C_6H_5), 7.57 (overlapping d, 6 H, *o*-C_6H_5). $^{13}C\{^1H\}$ NMR (C_6D_6, 25 °C, δ): 13.02 (C_5CH_3), 44.08 (SCH_2), 49.51 (SCH_2), 124.2 (C_5CH_3), 126.4, 127.4, 128.6, 129.0, 130.7 (C_6H_5), 141.2 (*i*-C_6H_5), 143.7 (*i*-C_6H_5). Anal. Calcd for $C_{62}H_{72}S_6Zr_2$: C, 62.37; H, 6.09. Found: C, 61.94; H, 6.32.

7. Yield: 90%.

7a. ^1H NMR (C_6D_6, 25 °C, δ): 1.32 (t, $|^3J_{H-H}|$ = 12.2 Hz, SCH_2CH_3); 1.34 (t, $|^3J_{H-H}|$ = 12.2 Hz, SCH_2CH_3); 2.08 (s, C_5CH_3); 2.98 (d of q, $|^2J_{H-H}|$ = 7.4 Hz, $|^3J_{H-H}|$ = 12.2 Hz, SCH_2); 3.21 (d of q, $|^2J_{H-H}|$ = 7.4 Hz, $|^3J_{H-H}|$ = 12.2 Hz, SCH_2); 3.51 (q, $|^3J_{H-H}|$ = 12.2 Hz, μ_2-SCH_2). $^{13}C\{^1H\}$ NMR (C_6D_6, 25 °C, δ): 13.3 (C_5CH_3); 19.2 (SCH_2CH_3) 20.7 (SCH_2CH_3); 29.7 (SCH_2); 36.5 (SCH_2); 124.8 (C_5CH_3).

7b. ^1H NMR (C_6D_6, 25 °C, δ): 1.49 (t, $|^3J_{H-H}|$ = 12.6 Hz, SCH_2CH_3); 1.50 (t, $|^3J_{H-H}|$ = 12.7 Hz, SCH_2CH_3); 1.52 (t, $|^3J_{H-H}|$ = 12.8 Hz, SCH_2CH_3); 2.12 (s, C_5CH_3); 3.43 (d of q, $|^2J_{H-H}|$ = 7.2 Hz, $|^3J_{H-H}|$ = 12.8 Hz, SCH_2); 3.48 (d of q, $|^2J_{H-H}|$ = 7.4 Hz, $|^3J_{H-H}|$ = 12.6 Hz, SCH_2); 3.56 (d of q, $|^2J_{H-H}|$ = 7.2 Hz, $|^3J_{H-H}|$ = 12.8 Hz, SCH_2); 3.63 (d of q, $|^2J_{H-H}|$ = 7.4 Hz, $|^3J_{H-H}|$ = 12.7 Hz, SCH_2); 3.67 (d of q, $|^2J_{H-H}|$ = 7.4 Hz, $|^3J_{H-H}|$ = 12.6 Hz, SCH_2); 3.76 (d of q, $|^2J_{H-H}|$ = 7.4 Hz, $|^3J_{H-H}|$ = 12.7 Hz, SCH_2). $^{13}C\{^1H\}$ NMR (C_6D_5, 25 °C, δ): 13.3 (C_5CH_3); 19.8 (SCH_2CH_3); 20.4 (SCH_2CH_3); 31.0 (SCH_2); 34.0 (SCH_2); 40.7 (SCH_2); 123.3 (C_5CH_3).

7c. ^1H NMR (C_6D_6, 25 °C, δ): 1.25 (t, $|^3J_{H-H}|$ = 12.9 Hz, SCH_2CH_3); 1.28 (t, $|^3J_{H-H}|$ = 12.9 Hz, SCH_2CH_3); 1.29 (t, $|^3J_{H-H}|$ = 13.6 Hz, SCH_2CH_3); 2.09 (s, C_5CH_3); 2.11 (s, C_5CH_3); 3.10 (d of q, $|^2J_{H-H}|$ = 7.5 Hz, $|^3J_{H-H}|$ = 12.9 Hz, SCH_2); 3.12 (d of q, $|^2J_{H-H}|$ = 7.4 Hz, $|^3J_{H-H}|$ = 12.9 Hz, SCH_2); 3.18 (d of q, $|^2J_{H-H}|$ = 7.5 Hz, $|^3J_{H-H}|$ = 13.0 Hz, SCH_2); 3.61 (d of q, $|^2J_{H-H}|$ = 7.4 Hz, $|^3J_{H-H}|$ = 12.9 Hz, SCH_2); 3.67 (d of q, $|^2J_{H-H}|$ = 7.5 Hz, $|^3J_{H-H}|$ = 12.9 Hz, SCH_2); 3.73 (d of q, $|^2J_{H-H}|$ = 7.5 Hz, $|^3J_{H-H}|$ = 13.0 Hz, SCH_2). $^{13}C\{^1H\}$ NMR (C_6D_6, 25 °C, δ): 13.3 (C_5CH_3); 19.3 (SCH_2CH_3); 28.5 (SCH_2); 41.4 (SCH_2); 123.4 (C_5CH_3); 124.6 (C_5CH_3). Anal. Calcd for $C_{32}H_{60}S_6Zr_2$: C, 46.89; H, 7.38. Found: C, 47.12; H, 7.16.

Generation of $Cp^*Zr(SBz)_3(PMe_3)$ (8). **6** (0.013 g, 0.022 mmol) was placed in an NMR tube and dissolved in benzene-d_6 (0.5 mL). PMe_3 (11 μL, 0.11 mmol) was added via a microliter syringe, and the reaction was monitored by ^1H and ^{31}P NMR. After 48 h no evidence of **6** was observed. Although the yield of **8** was greater than 95% by NMR, attempts to isolate **8** were unsuccessful. Data for **8** are as follows. ^1H NMR (C_6D_6, 25 °C, δ): 1.10 (d, $|^2J_{P-H}|$ = 13.3 Hz, 9H, PCH_3), 2.17 (s, 15H, C_5CH_3), 4.41 (d, $|^2J_{H-H}|$ = 13.7 Hz, 2H, SCH_2), 4.51 (d, $|^2J_{H-H}|$ = 13.7 Hz, 2H, SCH_2), 5.00 (s, 2H, SCH_2), 7.04 (m, 3H, *m,p*-C_6H_5), 7.19 (m, 6H, *m,p*-C_6H_5), 7.58 (d, $|^3J_{H-H}|$ = 7.3 Hz, 4H, *o*-C_6H_5), 7.68 (d, $|^3J_{H-H}|$ = 7.1 Hz, 2H, *o*-C_6H_5). $^{31}P\{^1H\}$ NMR (C_6D_6, 25 °C, δ): 61.6. $^{13}C\{^1H\}$ NMR (C_6D_6, 25 °C, δ): 12.61 (C_5CH_3), 22.41 (d, $|^1J_{P-C}|$ = 58.0 Hz, PCH_3), 39.82 (SCH_2), 41.82 (SCH_2), 122.2 (C_5CH_3), 125.9, 126.2, 127.1, 128.5, 128.8, 129.0 (C_6H_5), 144.6 (*i*-C_6H_5), 145.8 (*i*-C_6H_5).

Synthesis of $[Cp^*Zr(OMe)_2(\mu_2\text{-}OMe)]_2$ (9). **6** (0.15 g, 0.25 mmol) was dissolved in benzene (15 mL), and MeOH (0.06 mL, 1.48 mmol) was added via syringe. The solution immediately became colorless. After being stirred for 0.5 h, the volatiles were removed, and the white residue was recrystallized from hexane by slow evaporation in 95% yield. Data for **9** are as follows. ^1H NMR (C_6D_6, 25 °C, δ): 2.03 (s, 15 H, C_5CH_3), 3.58 (s, 3 H, μ_2-OCH_3), 4.08 (s, 6 H, OCH_3). $^{13}C\{^1H\}$ NMR (C_6D_6, 25 °C, δ): 10.61 (C_5CH_3), 56.60 (OCH_3), 57.33 (OCH_3), 119.3 (C_5CH_3). Anal. Calcd for $C_{26}H_{48}O_6Zr_2$: C, 48.86; H, 7.57. Found: C, 48.58; H, 7.49.

Synthesis of $[Cp^*Zr(SBz)]_2(\mu_2\text{-}SBz)_2(\mu_3\text{-}SBz)(\mu_3\text{-}O)Li(THF)$ (10). (i) Cp^*ZrCl_3·LiCl (0.105 g, 0.28 mmol) and NaSBz (0.137 g, 0.937 mmol), made from Na and wet benzyl mercaptan in THF, was placed in a flask, and benzene (15 mL) was added. After being stirred for 18 h, the yellow mixture was filtered, washed with benzene (3 × 5 mL), and stripped to dryness. The yellow residue was taken up in hexane, and crystallization by slow evaporation afforded **10** in 45% yield. (ii) Alternatively, the analogous reaction of Cp^*ZrCl_3 (0.17 g, 0.52 mmol), NaSBz (0.19 g, 1.3 mmol), and LiOH (0.006 g, 0.25 mmol) in THF (15 mL) provided **10** by ^1H NMR spectroscopy. ^1H NMR (C_6D_6, 25 °C, δ): 1.19 (m, 4H, THF), 2.13 (s, 30H, C_5Me_5), 3.47 (m, 4H, THF), 4.31 (m, 2H, SCH_2), 4.63 (m, 8H, SCH_2), 7.02 (m, 9H, Ph), 7.10 (m, 6H, Ph), 7.27 (m, 4H, Ph), 7.69 (m, 6H, Ph). Anal. Calcd for $C_{59}H_{73}LiO_2S_2Zr_2$: C, 60.89; H, 6.32. Found: C, 60.73; H, 6.50.

Molecular Modeling Calculations.[17] Energy minimization calculations were performed by employing the MMX and MM2 options of the Cache Software system operating on a Power Mac 7100 computer. Initial coordinates and geometric parameters were taken from X-ray data.

Extended Huckel Molecular Orbital Calculations.[17] EHMO calculations were performed by employing the adaptation of FORTICON-8 inherent in the Cache Software. Models were constructed by making suitable simplifications to the structures of **7** and **9**. In these cases initial Cartesian coordinates were used from the X-ray data. For calculations involving simple three-coordinate piano stool complexes, geometries were initially optimized on the basis of molecular mechanics energy minimizations.

X-ray Data Collection and Reduction. Crystals of **7b**, **9**, and **10** of suitable quality for X-ray diffraction experiments were obtained directly from the preparation as described above. The crystals were manipulated and mounted in capillaries in a glovebox, thus maintaining a dry, O_2-free environment for each crystal. Diffraction experiments were performed on a Rigaku AFC6 diffractometer equipped with graphite-monochromatized Mo Kα radiation. The initial orientation matrices were obtained from 20 machine-centered reflections selected by an automated peak search routine. These data were used to determine the crystal systems. Automated Laue system check routines around each axis were consistent with the crystal system. Ultimately, 25 reflections ($20° < 2\theta < 25°$) were used to obtain the final lattice parameters and the orientation matrices. Crystal data are summarized in Table 1. The observed symmetry and extinctions (where appropriate) were consistent with the space groups. The data sets were collected in four shells ($4.5° < 2\theta < 50.0°$), and three standard reflections were recorded every 197 reflections. Fixed scan rates were employed. Up to 4 repetitive scans of each reflection at the respective scan rates were averaged to ensure meaningful statistics. The number of scans of each reflections was determined by the intensity. The intensities of the standards showed no statistically significant change over the duration of the data collection. The data were processed using the TEXSAN crystal solution package operating on a Silicon Graphics workstation employing remote X-terminals. The reflections with $F_o^2 > 3\sigma(F_o^2)$ were used in the refinements.

Structure Solution and Refinement. Non-hydrogen atomic scattering factors were taken from the literature tabulations.[18,19] The Zr

(17) CaChe Worksystem Software is an integrated modeling, molecular mechanics and molecular orbital computational software package and is a product of CaChe Scientific Inc.

Table 1. Crystallographic Parameters for **7b**, **9**, and **10**

	7b	**9**	**10**
formula	$C_{32}H_{60}S_6Zr_2$	$C_{26}H_{48}O_6Zr_2$	$C_{59}H_{73}LiO_2S_5Zr_2$
fw	409.81	319.55	1163.91
cryst system	triclinic	monoclinic	triclinic
space group	$P\bar{1}$	$P2_1/n$	$P\bar{1}$
a (Å)	9.580(3)	12.540(3)	12.907(8)
b (Å)	12.210(2)	9.694(3)	22.270(6)
c (Å)	9.222(3)	13.165(3)	11.610(8)
α (deg)	95.01(2)		99.81(3)
β (deg)	108.55(2)	107.16(2)	114.59(6)
γ (deg)	72.62(2)		79.24(3)
V (Å^3)	976.0(5)	1529.3(7)	2965(3)
Z	1	2	2
μ (cm^{-1})	8.74	7.14	5.66
d(calc) (g/cm^3)	1.39	1.39	1.30
λ (Å), radiation	0.710 69, Mo Kα	0.710 69, Mo Kα	0.710 69, Mo Kα
T (°C)	24	24	24
R (%)[a]	4.5	4.2	7.8
R_w (%)[a]	4.7	3.2	8.3

[a] $R = \sum||F_o| - |F_c||/\sum|F_o|$; $R_w = [\sum(|F_o| - |F_c|)^2/\sum|F_o|^2]^{0.5}$.

atom positions were determined using direct methods employing either the SHELX-86 or Mithril direct methods routines. The remaining non-hydrogen atoms were located from successive difference Fourier map calculations. The refinements were carried out by using full-matrix least-squares techniques on F, minimizing the function $\omega(|F_o| - |F_c|)^2$, (where the weight ω was defined as $4F_o^2/2\sigma(F_o^2)$ and F_o and F_c were the observed and calculated structure factor amplitudes. In the final cycles of the refinements all non-hydrogen atoms in **7b** and **9** were assigned anisotropic temperature factors. In the case of **10** the Zr, S, O, and methylene carbon atoms were refined anisotropically with the remainder of the carbon atoms being refined isotropically. This was done in order to maintain a reasonable data:variable ratio. Empirical absorption corrections were applied to the data on the basis of ψ-scan data and employing the software resident in the TEXSAN package. Hydrogen atom positions were calculated and allowed to ride on the carbon to which they are bonded by assuming a C−H bond length of 0.95 Å. Hydrogen atom temperature factors were fixed at 1.10 times the isotropic temperature factor of the carbon atom to which they are bonded. The hydrogen atom contributions were calculated but not refined. The final values of R and R_w are given in Table 1. The maximum Δ/σ on any of the parameters in the final cycles of the refinement and the location of the largest peaks in the final difference Fourier map calculation are also given in Table 1. The residual electron densities in each case were of no chemical significance. The following data are tabulated: selected positional parameters (Table 2) and selected bond distances and angles (Table 3). Crystallographic parameters, hydrogen atom parameters (Table S1), thermal parameters (Table S2), and bond distances and angles (Table S3) have been deposited as supplementary material.

Results

Synthesis. The reaction of a slight excess of 3 equiv of sodium benzyl mercaptan with Cp^*ZrCl_3 proceeds at 25 °C in benzene over an 18 h period. The yellow reaction mixture is filtered, the solvent is removed *in vacuo*, and hexane is added to the oily residue. This results in the formation of a yellow powdery precipitate **6**. The ^{1}H NMR spectrum of **6** exhibits resonances at 7.06, 5.11, 4.76, 4.82, and 1.97 ppm attributable to the phenyl, methylene, and methyl groups, respectively. The ratio of the integrals of the methylene and methyl resonances in the ^{1}H NMR spectrum is consistent with complete replacement of the chlorides of Cp^*ZrCl_3 with thiolate ligands. However, the observation of two types of methylene resonances in both the ^{1}H and ^{13}C{^{1}H} NMR spectra as well as the 2:1 ratio of the integrals in the ^{1}H NMR spectrum infers the presence of both bridging and terminal thiolate ligands. The lower field, more intense, methylene resonance is an AB doublet of doublets consistent with inequivalent geminal protons while the higher field resonance is a singlet. These resonances are attributed to the terminal and bridging thiolate ligands, respectively, and are consistent with a symmetric dimer in which two thiolate ligands bridge two Zr centers. Furthermore, for such dimeric formulations the pentamethylcyclopentadienyl ligands may adopt either a *cisoid* or *transoid* disposition. The latter would yield inequivalent methylene protons in the bridging thiolate moieties, and thus, the data for **6** are consistent with the *cisoid* isomer geometry.

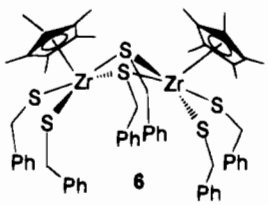

6

The analogous reaction of sodium ethanethiolate and Cp^*ZrCl_3 proceeds in a similar fashion. Slow evaporation of solvent from hexane solution of **7** affords crystalline material. The ^{1}H NMR spectrum of **7** as isolated in this manner is quite complex. Four resonances arise from the pentamethylcyclopentadienyl ligands while a number of overlapping resonances are observed for the methylene and eight methyl protons. Integration data are consistent with complete replacement of chloride with ethanethiolate ligands, although the spectral complexity infers the presence of several isomers of dimers. Similarly, the ^{13}C{^{1}H} NMR spectrum of **7** exhibits overlapping sets of methylene and methyl resonances in addition to the four resonances attributed to the inner ring carbons of the Cp* ligands. These data are consistent with a mixture of three isomers of the dimeric species **7**: *cisoid* (*syn*) **7a**, *transoid* (*anti*) **7b**, and *transoid* (*syn*) **7c** (Chart 2). Repeated recrystallizations allow the isolation of samples of **7** enriched in one isomer as well as crystals suitable for X-ray analysis. ^{1}H and ^{13}C{^{1}H} NMR spectra of these mixtures, in conjunction with high-field (500 MHz) 1D and 2D ^{1}H NMR data (Figures 1 and 2), permitted the rigorous assignment of the spectral parameters for each isomer. In the case of **7c**, the Cp* ligands are inequivalent and give rise to the central pair of Cp* methyl resonances in the ^{1}H NMR spectrum. A ^{1}H NMR spectrum of the crystals used for structural analysis allowed the assignment of the resonances attributed to **7b**; thus, the low-field Cp* resonance arises from **7b**. The remaining resonances in NMR spectra of the mixture of isomers of **7** were assigned to **7a**. No evidence of interconversion of the isomers of **7** was observed. Examination of the ^{1}H NMR spectra of **7** as a function of temperature revealed some line broadening as well as some slight changes in the positions of the Cp*-methyl resonances at −80 °C, although no coalescence of resonances was observed. In addition, the spectra data from samples of crystallized batches of **7** which were successively enriched in **7b** indicate that there is no low-energy process for the interconversion of the isomers of **7**. Heating a benzene-d_6 solution of **7** to 60°C resulted in no change in the ratio of isomers although prolonged heating resulted in decomposition.

Reaction of **6** with PMe_3 was monitored by ^{31}P{^{1}H} NMR spectroscopy. In the presence of 1 equiv of phosphine no apparent reaction was indicated after 12 h. However, in the presence of 5 equiv of PMe_3 reaction slowly proceeded over a

(18) (a) Cromer, D. T.; Mann, J. B. *Acta Crystallogr. Sect. A: Cryst. Phys., Theor. Gen. Crystallogr.* **1968**, *A24*, 324. (b) *Ibid.* **1968**, *A24*, 390.
(19) Cromer, D. T.; Waber, J. T. *International Tables for X-ray Crystallography*; Kynoch Press: Birmingham, England, 1974.

Table 2. Positional Parameters

atom	*x*	*y*	*z*	atom	*x*	*y*	*z*
			Compound **7b**				
Zr(1)	0.90146(7)	0.68791(5)	0.45987(7)	C(7)	0.7001(8)	0.9874(6)	0.4900(9)
S(1)	1.0464(2)	0.8139(1)	0.6238(2)	C(8)	0.7442(8)	0.8248(6)	0.7621(8)
S(2)	0.9776(2)	0.7105(2)	0.2325(2)	C(9)	0.6582(8)	0.5955(6)	0.615(1)
S(3)	0.9276(2)	0.4759(1)	0.3421(2)	C(10)	0.5366(8)	0.6294(7)	0.261(1)
C(1)	0.6300(7)	0.8122(6)	0.3346(8)	C(11)	1.2475(8)	0.7468(6)	0.6407(9)
C(2)	0.6867(7)	0.8667(5)	0.4749(8)	C(12)	1.348(1)	0.7725(8)	0.795(1)
C(3)	0.7076(7)	0.7937(5)	0.5969(7)	C(13)	0.981(1)	0.8574(6)	0.213(1)
C(4)	0.6641(7)	0.6953(5)	0.5306(8)	C(14)	1.098(1)	0.8619(8)	0.146(1)
C(5)	0.6164(7)	0.7062(5)	0.3712(8)	C(15)	0.9250(8)	0.4421(6)	0.1449(7)
C(6)	0.5762(8)	0.8650(7)	0.1792(9)	C(16)	0.773(1)	0.4837(8)	0.0281(8)
			Compound **9**				
Zr(1)	0.08551(7)	0.05478(9)	0.41912(7)	C(6)	0.2599(9)	0.077(1)	0.2593(9)
O(1)	0.2027(5)	0.1826(6)	0.4948(5)	C(7)	0.0178(8)	−0.040(1)	0.1469(6)
O(2)	0.0135(5)	0.1974(6)	0.3171(5)	C(8)	−0.0356(8)	−0.271(1)	0.2970(8)
O(3)	−0.0831(4)	0.0087(5)	0.4230(4)	C(9)	0.1708(8)	−0.3008(9)	0.4984(7)
C(1)	0.1990(7)	−0.030(1)	0.3043(7)	C(10)	0.3577(7)	−0.088(1)	0.4771(7)
C(2)	0.0916(8)	−0.081(1)	0.2554(6)	C(11)	0.269(1)	0.291(1)	0.516(1)
C(3)	0.0675(7)	−0.181(1)	0.3219(7)	C(12)	−0.001(1)	0.322(1)	0.278(1)
C(4)	0.1607(7)	−0.1949(8)	0.4131(7)	C(13)	−0.1805(7)	0.019(1)	0.3340(6)
C(5)	0.2426(7)	−0.1014(9)	0.4023(7)				
			Compound **10**				
Zr(1)	0.7588(2)	0.22567(9)	0.1024(2)	C(27)	0.998(2)	0.412(1)	0.096(2)
Zr(2)	0.5864(2)	0.1579(1)	−0.2102(2)	C(28)	0.557(2)	0.362(1)	0.019(2)
S(1)	0.8467(5)	0.3046(3)	0.0500(6)	C(29)	0.484(2)	0.4176(9)	0.056(2)
S(2)	0.6185(5)	0.3125(2)	0.1499(5)	C(30)	0.371(2)	0.425(1)	−0.010(2)
S(3)	0.8118(5)	0.1641(2)	−0.0903(5)	C(31)	0.302(2)	0.478(1)	0.021(3)
S(4)	0.5753(5)	0.2201(2)	0.3755(5)	C(32)	0.356(2)	0.518(1)	0.112(2)
S(5)	0.4033(5)	0.2226(3)	−0.2020(5)	C(33)	0.468(2)	0.516(1)	0.177(2)
O(1)	0.626(1)	0.1763(6)	−0.016(1)	C(34)	0.538(2)	0.464(1)	0.149(2)
O(2)	0.396(2)	0.224(1)	0.103(2)	C(35)	0.884(2)	0.200(1)	−0.162(2)
C(1)	0.799(2)	0.147(1)	0.255(2)	C(36)	0.951(2)	0.157(1)	−0.226(2)
C(2)	0.774(2)	0.203(1)	0.317(2)	C(37)	1.037(2)	0.112(1)	−0.163(2)
C(3)	0.865(2)	0.238(1)	0.347(2)	C(38)	1.101(2)	0.072(1)	−0.221(3)
C(4)	0.939(2)	0.203(1)	0.296(2)	C(39)	1.076(3)	0.073(1)	−0.348(3)
C(5)	0.901(2)	0.146(1)	0.239(2)	C(40)	0.992(3)	0.118(1)	−0.407(3)
C(6)	0.724(2)	0.095(1)	0.219(2)	C(41)	0.933(2)	0.159(1)	−0.347(2)
C(7)	0.682(2)	0.224(1)	0.367(2)	C(42)	0.584(2)	0.299(1)	−0.296(2)
C(8)	0.883(2)	0.297(1)	0.428(2)	C(43)	0.595(2)	0.3414(9)	−0.377(2)
C(9)	1.053(2)	0.220(1)	0.312(2)	C(44)	0.701(2)	0.359(1)	−0.340(2)
C(10)	0.962(2)	0.093(1)	0.191(3)	C(45)	0.721(2)	0.399(1)	−0.410(3)
C(11)	0.643(2)	0.043(1)	−0.239(3)	C(46)	0.628(2)	0.421(1)	−0.511(2)
C(12)	0.629(2)	0.061(1)	−0.352(2)	C(47)	0.523(2)	0.404(1)	−0.546(2)
C(13)	0.516(2)	0.083(1)	−0.412(3)	C(48)	0.504(2)	0.366(1)	−0.476(2)
C(14)	0.459(2)	0.075(1)	−0.334(3)	C(49)	0.288(2)	0.248(1)	−0.344(2)
C(15)	0.543(3)	0.053(1)	−0.229(3)	C(50)	0.203(2)	0.303(1)	−0.314(2)
C(16)	0.739(4)	0.007(2)	−0.139(5)	C(51)	0.144(3)	0.293(1)	−0.252(3)
C(17)	0.749(4)	0.050(2)	−0.372(5)	C(52)	0.065(3)	0.341(2)	−0.218(3)
C(18)	0.514(4)	0.093(2)	−0.544(4)	C(53)	0.074(3)	0.393(1)	−0.256(3)
C(19)	0.336(4)	0.095(2)	−0.427(5)	C(54)	0.128(3)	0.409(1)	−0.318(3)
C(20)	0.477(4)	0.042(2)	−0.153(4)	C(55)	0.205(3)	0.358(2)	−0.344(3)
C(21)	0.860(2)	0.376(1)	0.160(2)	C(56)	0.325(3)	0.180(2)	0.076(4)
C(22)	0.973(2)	0.400(1)	0.194(2)	C(57)	0.244(5)	0.200(3)	0.132(6)
C(23)	1.043(3)	0.416(1)	0.319(3)	C(58)	0.276(4)	0.258(2)	0.200(5)
C(24)	1.148(2)	0.440(1)	0.342(3)	C(59)	0.353(3)	0.275(2)	0.160(4)
C(25)	1.163(3)	0.449(1)	0.244(3)	Li(1)	0.497(3)	0.233(2)	0.033(4)
C(26)	1.098(3)	0.438(1)	0.122(3)				

2 day period. In the presence of larger excesses of phosphine (30 equiv) NMR data were consistent with the complete formation of the monomer phosphine adduct $Cp^*Zr(SBz)_3(PMe_3)$ (**8**) in 12 h. The requirement of a large excess of phosphine for a discernible reaction suggests a dimer−monomer equilibria (eq 1) between **6** and **8**. This view is also consistent with the observation of the reformation of **6** upon placement of solutions of **8** under vacuum.

$$\underset{\mathbf{6}}{[Cp^*Zr(SR)_2(\mu\text{-}SR)_2]} + PMe_3 \rightleftharpoons \underset{\mathbf{8}}{Cp^*Zr(SR)_3(PMe_3)} \quad (1)$$

Reaction of **6** with 6 equiv of MeOH in benzene proceeds rapidly. In a matter of minutes the initial yellow color is dissipated. Recrystallization of the resulting product from hexanes affords the crystalline material **9**. The liberation of free thiol was confirmed by NMR data for the reaction mixture. The ^1H and $^{13}C\{^1H\}$ NMR spectra of isolated product **9** exhibit resonances attributable to a single pentamethylcyclopentadienyl ligand environment as well as bridging and terminal methoxide ligands. A dimeric formulation was suggested (eq 2). Unlike

$$\underset{\mathbf{6}}{[Cp^*Zr(SR)_2(\mu\text{-}SR)_2]} + 6MeOH \rightarrow \underset{\mathbf{9}}{[Cp^*Zr(OMe)_2(\mu\text{-}OMe)_2]} + 6HSR \quad (2)$$

the thiolate complexes **6** or **7**, the NMR data for **9** do not

Table 3. Selected Bond Distances (Å) and Angles (deg)

	Compound **7b**		
	Distances		
Zr(1)−S(1)	2.472(2)	Zr(1)−S(2)	2.489(2)
Zr(1)−S(3)	2.691(2)	Zr(1)−S(3)	2.607(2)
Zr(1)−C(1)	2.537(6)	Zr(1)−C(2)	2.542(6)
Zr(1)−C(3)	2.547(6)	Zr(1)−C(4)	2.533(6)
Zr(1)−C(5)	2.534(6)	S(1)−C(11)	1.816(7)
S(2)−C(13)	1.827(8)	S(3)−C(15)	1.824(6)
	Angles		
S(1)−Zr(1)−S(2)	94.31(6)	S(1)−Zr(1)−S(3)	144.09(6)
S(1)−Zr(1)−S(3)	87.29(6)	S(2)−Zr(1)−S(3)	79.91(5)
S(2)−Zr(1)−S(3)	119.84(6)	S(3)−Zr(1)−S(3)	66.18(6)
Zr(1)−S(1)−C(11)	106.7(2)	Zr(1)−S(2)−C(13)	111.6(3)
Zr(1)−S(3)−Zr(1)	113.82(6)	Zr(1)−S(3)−C(15)	123.5(2)
Zr(1)−S(3)−C(15)	115.1(2)		
	Compound **9**		
	Distances		
Zr(1)−O(1)	1.955(6)	Zr(1)−O(2)	1.953(6)
Zr(1)−O(3)	2.176(5)	Zr(1)−O(3)	2.177(4)
Zr(1)−C(1)	2.500(7)	Zr(1)−C(2)	2.546(8)
Zr(1)−C(3)	2.593(8)	Zr(1)−C(4)	2.607(7)
Zr(1)−C(5)	2.546(8)	O(1)−C(11)	1.32(1)
O(2)−C(12)	1.30(1)	O(3)−C(13)	1.424(8)
	Angles		
O(1)−Zr(1)−O(2)	91.6(3)	O(1)−Zr(1)−O(3)	135.0(2)
O(1)−Zr(1)−O(3)	85.0(2)	O(2)−Zr(1)−O(3)	84.6(2)
O(2)−Zr(1)−O(3)	136.3(2)	O(3)−Zr(1)−O(3)	68.4(2)
Zr(1)−O(1)−C(11)	160.8(8)	Zr(1)−O(2)−C(12)	155.5(8)
Zr(1)−O(3)−Zr(1)	111.6(2)	Zr(1)−O(3)−C(13)	124.8(4)
Zr(1)−O(3)−C(13)	123.7(4)		
	Compound **10**		
	Distances		
Zr(1)−S(1)	2.535(6)	Zr(1)−S(2)	2.546(6)
Zr(1)−S(3)	2.689(6)	Zr(1)−O(1)	2.07(1)
Zr(1)−C(1)	2.54(2)	Zr(1)−C(2)	2.54(2)
Zr(1)−C(3)	2.58(2)	Zr(1)−C(4)	2.51(2)
Zr(1)−C(5)	2.52(2)	Zr(2)−S(3)	2.671(6)
Zr(2)−S(4)	2.496(6)	Zr(2)−S(5)	2.558(6)
Zr(2)−O(1)	2.08(1)	Zr(2)−C(11)	2.53(3)
Zr(2)−C(12)	2.60(2)	Zr(2)−C(13)	2.57(2)
Zr(2)−C(14)	2.54(3)	Zr(2)−C(15)	2.46(3)
S(1)−C(21)	1.85(2)	S(2)−C(28)	1.84(2)
S(3)−C(35)	1.83(2)	S(4)−C(42)	1.84(2)
S(5)−C(49)	1.79(2)	S(2)−Li(1)	2.43(4)
S(5)−Li(1)	2.47(4)	O(1)−Li(1)	2.10(4)
O(2)−Li(1)	1.86(4)	O(2)−C(56)	1.37(3)
O(2)−C(59)	1.36(4)	Zr(1)−Li(1)	3.11(4)
	Angles		
S(1)−Zr(1)−S(2)	88.8(2)	S(1)−Zr(1)−S(3)	78.0(2)
S(1)−Zr(1)−O(1)	129.5(4)	S(2)−Zr(1)−S(3)	142.0(2)
S(2)−Zr(1)−O(1)	91.1(4)	S(3)−Zr(1)−O(1)	71.6(3)
S(3)−Zr(2)−S(4)	90.2(2)	S(3)−Zr(2)−S(5)	136.0(2)
S(3)−Zr(2)−O(1)	71.8(3)	S(4)−Zr(2)−S(5)	89.4(2)
S(4)−Zr(2)−O(1)	133.5(4)	S(5)−Zr(2)−O(1)	76.9(3)
Zr(1)−S(1)−C(21)	113.0(7)	Zr(1)−S(2)−C(28)	108.7(7)
Zr(1)−S(2)−Li(1)	77(1)	C(28)−S(2)−Li(1)	95(1)
Zr(1)−S(3)−Zr(2)	84.8(2)	Zr(1)−S(3)−C(35)	120.4(7)
Zr(2)−S(3)−C(35)	119.7(7)	Zr(2)−S(4)−C(42)	104.4(7)
Zr(2)−S(5)−C(49)	121.0(8)	Zr(2)−S(5)−Li(1)	89(1)
C(49)−S(5)−Li(1)	149(1)	Zr(1)−O(1)−Zr(2)	121.3(6)
Zr(1)−O(1)−Li(1)	96(1)	Zr(2)−O(1)−Li(1)	115(1)
C(56)−O(2)−C(59)	107(2)	C(56)−O(2)−Li(1)	131(3)
C(59)−O(2)−Li(1)	118(2)	S(2)−Li(1)−S(5)	121(2)
S(2)−Li(1)−O(1)	94(2)	S(2)−Li(1)−O(2)	113(2)
S(5)−Li(1)−O(1)	79(1)	S(5)−Li(1)−O(2)	111(2)
O(1)−Li(1)−O(2)	137(2)		

unambiguously distinguish between the possible geometries. X-ray data subsequently confirmed both the dimeric formulation and a *transoid* disposition of the pentamethylcyclopentadienyl ligands (*vide infra*). The ready displacement of thiolate by alkoxide is consistent with the oxophilicity of Zr. In the presence of less than 6 equiv of methanol, no evidence of mixed thiolate/alkoxide complexes was detected as only unreacted **6** and **9** are observed.

Further reactivity studies were undertaken. Compound **6** did not react with excess aniline. Thermolysis of **6** via heating at 60 °C overnight resulted in the formation of benzyl mercaptan, benzyl disulfide, and uncharacterized Zr byproducts. While it is conceivable that intramolecular C−H activation of a methyl group on the pentamethylcyclopentadienyl ligand constitutes a proton source, this remains unproven. Reaction of **6** with MeI at 60 °C in benzene accelerates the formation of $PhCH_2SMe$ that also occurs more slowly at 25 °C. Again the fate of the Zr is unknown.

In our early attempts to prepare **6**, it was found that some purchased Cp^*ZrCl_3 contained 1 equiv of LiCl presumably derived from the introduction of the Cp* ligand.[20] This, in combination with adventious water in the thiol, afforded the isolation of new yellow crystalline Zr-containing product **10** in low yield. The ^1H NMR spectrum of compound **10** revealed the presence of pentamethylcyclopentadienyl, bridging and terminal benzyl mercaptide ligands, and 1 equiv of THF. The nature of this product **10** was determined by X-ray crystallography to be $[Cp^*Zr(SBz)]_2(\mu_2\text{-}SBz)_3(\mu_3\text{-}O)Li(THF)$ (*vide infra*). Subsequently, it was found that use of purified starting materials and the rigorous exclusion of H_2O permitted the formation of **6** (*vide supra*). Furthermore, reaction of Cp^*ZrCl_3 with 0.5 equiv of LiOH in THF followed by addition of 2.5 equiv of NaSBz yields **10**.

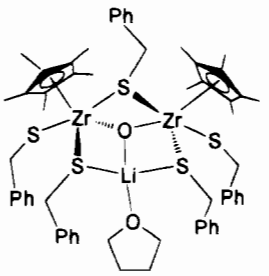

10

Structural Studies. Crystallographic study of compound **7b** confirms the dimeric structure in which two thiolate sulfur atoms bridge the two Zr centers (Figure 3). Two terminal thiolates and a η^5-pentamethylcyclopentadienyl ligand complete the coordination spheres of each of the Zr centers. Crystallographically the molecule is strictly centrosymmetric, and thus, only half of the dimer occupies the asymmetric unit. The geometry at Zr is thus best described as a pseudo-square-based pyramid or as a "four legged piano stool". The two η^5-pentamethylcyclopentadienyl ligands are *transoid* with respect to the Zr_2S_2 core. The terminal Zr−S distances are 2.472(2) and 2.489(3) Å, while the C−S−Zr angles in these fragments are 106.7(2) and 111.6(3)°. These distances compare with the terminal Zr−S_{avg} distances of 2.423(8) Å found in $Zr_3(S)(t\text{-}BuS)_{10}$[21] and 2.515(2) and 2.480(2) Å found in $[Cp_2Zr(SCH_2CH_2CH_2S)]_2$.[22] As expected, the bridging Zr−S distances of 2.691(2) and 2.607(2) Å in **7b** are dramatically longer. These bridging distances are similar to the average Zr−μ_2-thiolate sulfur distances of 2.617(7) Å and shorter than the average Zr−μ_3-thiolate distance (2.765(5) Å) found in $Zr_3(S)(t\text{-}BuS)_{10}$.[21] The geometry at the bridging sulfur is almost trigonal planar as the

(20) Huang, Y.; Stephan, D. W. Unpublished results.
(21) Coucouvanis, D.; Hadjikyriacou, A.; Lester, R.; Kanatzidis, M. G. *Inorg. Chem.* **1994**, *33*, 3645.
(22) (a) Stephan, D. W. *J. Chem. Soc., Chem. Commun.* **1991**, 121. (b) Stephan, D. W. *Organometallics* **1991**, *10*, 2037.

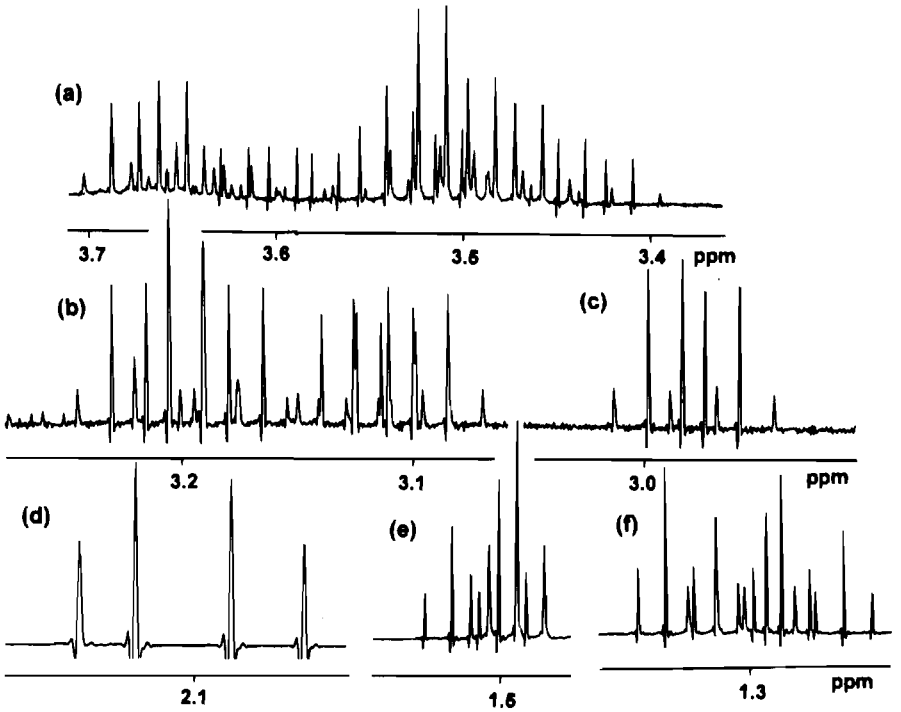

Figure 1. 500 MHz ^{1}H NMR spectrum of a mixture of the isomers of **7**. Key: (a–c) methylene proton resonances; (e, f) methyl resonances of ethyl groups; (d) Cp* methyl resonances.

Chart 2. Isomers of **7**: **7a**, *cisoid* (*syn*); **7b**, *transoid* (*anti*); **7c**, *transoid* (*syn*).

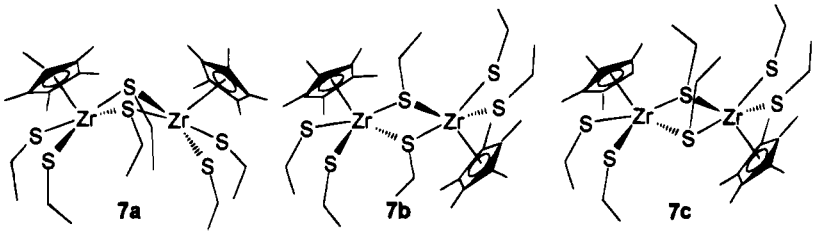

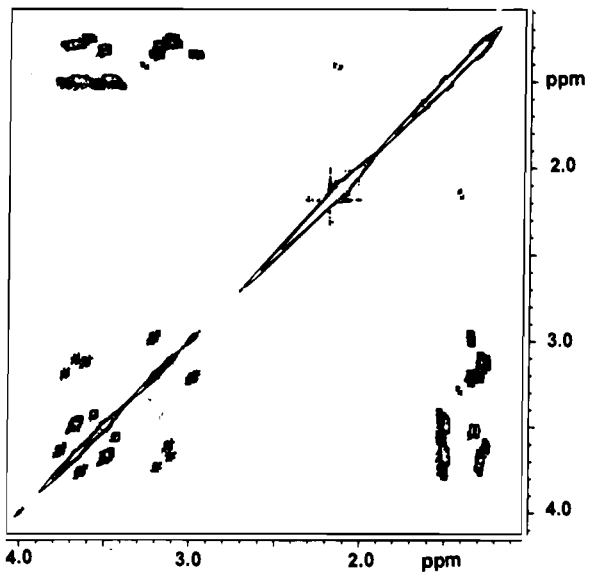

Figure 2. 2-D ^{1}H NMR spectrum of the mixture of the isomers of **7**.

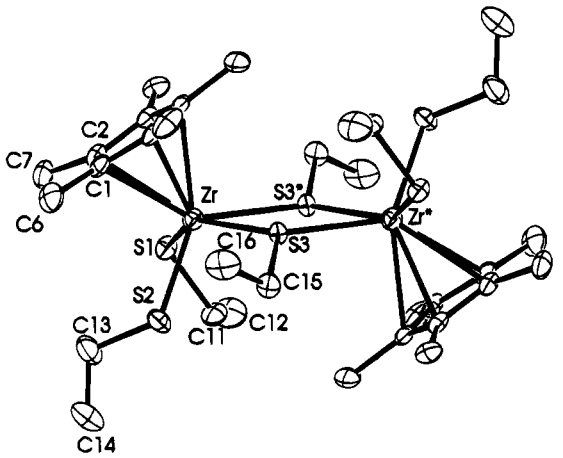

Figure 3. ORTEP drawing of **7b** with 30% thermal ellipsoids shown. All hydrogen atoms are omitted for clarity.

angles about S sum to 352.4°. The Zr_2S_2 core is strictly planar as a result crystallographically imposed symmetry. The S–Zr–S and Zr–S–Zr angles are 66.18(5) and 113.82(5)°, respectively, while the Zr··Zr distance is 4.438(1) Å. The remaining Zr–C, S–C, and C–C distances are typical.

Similar to **7b**, the crystallographic data for compound **9** reveal a symmetric dimer structure in which the pentamethylcyclopentadienyl groups are transoid and the Zr_2O_2 core is planar (Figure 4). The bridging alkoxide oxygen atoms give rise to Zr–O–Zr angles of 111.6(3)°, while the angles about O(3) sum to 360° indicating in a planar geometry. The bridging Zr–O distances average 2.176(5) Å. The terminal alkoxide oxygen atoms are almost linear as the corresponding C–O–Zr angles average 158.2(2)°. The terminal Zr–O bonds average 1.954(6) Å, which is comparable to that seen in $[Cp_2Zr(OCH_2CMe_2CH_2O)]_2$ (1.945(6) Å).[23] The O–Zr–O angle within the Zr_2O_2 core is 68.4(2)°, which is significantly less than the correspond-

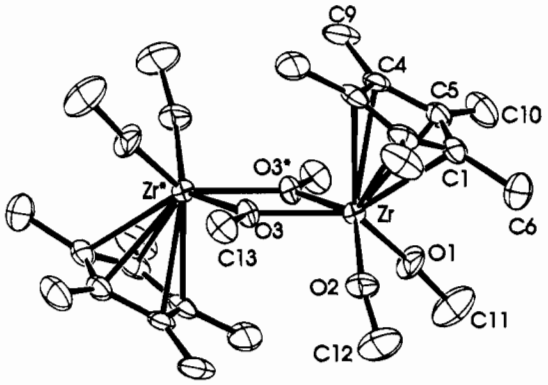

Figure 4. ORTEP drawing of **9** with 30% thermal ellipsoids shown. All hydrogen atoms are omitted for clarity.

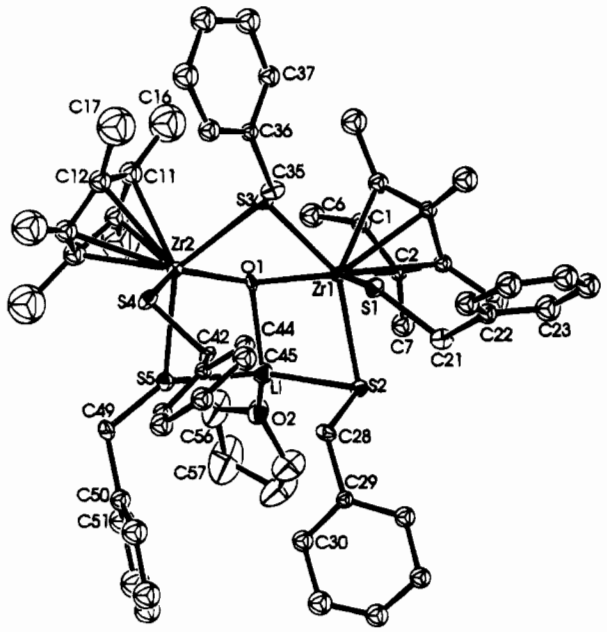

Figure 5. ORTEP drawing of **10** with 30% thermal ellipsoids shown. All hydrogen atoms are omitted for clarity.

ing angle of 101.4(3)° seen in $[Cp_2Zr(OCH_2CMe_2CH_2O)]_2$.[23] This results in a Zr··Zr distance of 3.600(2) Å.

Structural data for **10** reveal the compound consists of two (pentamethylcyclopentadienyl)zirconium fragments which are bridged by a single benzyl mercaptide ligand. In addition, a single terminal thiolate ligand resides on each Zr while two other thiolate ligands, one on each Zr atom, bridge to a single Li atom (Figure 5). A lone oxygen atom is triply bridging the two Zr centers and the Li. The coordination sphere of the Li is completed by a THF molecule. The two η^5-pentamethylcyclopentadienyl ligands are oriented on the same side of the Zr_2SO core and thus are described as *cisoid*. The terminal Zr−S bond lengths are 2.535(6) and 2.557(6) Å, while the Zr−S distances of the Zr−S−Zr bridge are 2.689(6) and 2.671(6) Å. These values are comparable to those seen in **7b**. In the Zr−S−Li bridges the Zr−S distances are 2.546(6) and 2.496(6) Å. These latter distances seem to suggest only a weak interaction of the thiolate sulfurs with lithium. The Zr−O distances in **10** are 2.07(1) and 2.08(1) Å, which are significantly shorter than the bridging alkoxide distances seen in **9**, consistent with the formal charge on the bridging O atom of **10**. The Zr_2SO core is not planar as the two ZrSO planes from a dihedral angle of 151.2(1)°. Both of the bridging chalcogenide atoms are pseudo-pyramidal as the angles sum to 332.3(1) and 324.9(1)° about O and S, respectively. The Li−S distances, which average 2.45(4) Å, further reflect the weak Li−S interaction. The remainder of the pseudo-tetrahedral coordination geometry about Li is completed by the μ_3-O atom which is positioned 2.10(1) Å from Li and a THF molecule at a Li−O distance of 1.86(4) Å.

EHMO Calculations. To further investigate the nature of these dimeric complexes, EHMO calculations[17] were performed on the model complexes $CpZr(EMe)_3$ (E = S (**11**), O (**12**)) and the *transoid* isomers of $[CpZr(EMe)_2(\mu\text{-}EMe)]_2$ (E = S (**13**), O (**14**)) (Chart 3). In the case of the monomeric species optimized geometries were obtained from molecular mechanics calculations. For the dimers, the coordinates for the models were derived from the X-ray data (*vide supra*). Calculations for **11** and **12** resulted in a description of the bonding which is similar to that previously described for $CpTi(SH)_3$.[14] The low-lying, vacant $1a_1$ and 1e orbitals for these monomeric d^0 Zr complexes are comprised primarily of metal-based d_{z^2}, d_{xy}, and $d_{x^2-y^2}$ atomic orbitals. In the case of **12**, the optimized geometry employed in the calculations is 3-fold symmetric and consequently the 2 1e orbitals are energetically degenerate. In contrast, a small separation in energy was observed for the 1e orbitals of **11** arising from the absence of symmetry in the optimized geometry. The HOMOs of these monomers are also dissimilar from each other. In the case of **11** the HOMOs are three energetically degenerate orbitals which are essentially lone pairs of electrons on the sulfur atoms. In contrast, the lone pairs on the oxygen atoms of **12** are lower in the manifold of molecular orbitals and two orbitals associated with the Cp ligands are the degenerate HOMOs.

MO calculations for the *transoid* dimers **13** and **14** reveal that bonding in the dimers is simply understood. In the case of **13** the pairwise combination of HOMO and LUMOs from two monomers results in the bridging Zr−S bonds (Figures 6 and 7). Despite the fact that the lone pairs on oxygen are not the HOMOs of **12**, a similar mix of the LUMO with the lone pairs on oxygen results in the formation of **14**.

A further aspect of these dimers to consider is Zr−E π-bonding. The vacant or frontier orbitals of the monomers **11** and **12** are metal-based d orbitals described above. Neither the $1a_1$ or 1e orbitals are of the proper symmetry to result in a π-interaction with the lone pair of electrons on the bridging O or S atoms that are present in the dimers. This is consistent with the characterization of the HOMOs of **13** which are comprised primarily as p_z orbitals on S. These orbitals are orthogonal to the Zr_2S_2 core and thus preclude a π-bonding interaction with the vacant d orbital which is parallel to the cyclopentadienyl ring. The same symmetry considerations apply to the bridging oxygen atoms of **14**. In contrast, the terminal chalcogenide atoms may adopt an orientation which permits an orbital containing a lone pair of electrons to be coplanar with a vacant 1e orbital on Zr. The degree of mixing of these orbitals would determine the degree of π-bonding. In the case of **9** such an interaction appears significant as evidenced by the short terminal Zr−O distance and the large Zr−O−C angle. Analogous π-bonding in **7b** appears much weaker as indicated by the metric parameters discussed above. These views are consistent with notions of the propensity of Zr for π-interactions with alkoxides and thiolates previously reported for metallocene derivatives.

EHMO calculations for the *cisoid* isomers **15** and **16** of the dimers reflect bonding akin to that described for the *transoid* isomers. In a similar fashion, the lone pairs of electrons on the bridging oxygen or sulfur atoms do not interact with the vacant d-orbitals on Zr, despite the puckering of the Zr_2E_2 core. One is left with the conclusion that the puckering of the core is a

(23) Stephan, D. W. *Organometallics* **1990**, *9*, 2718.

Chart 3

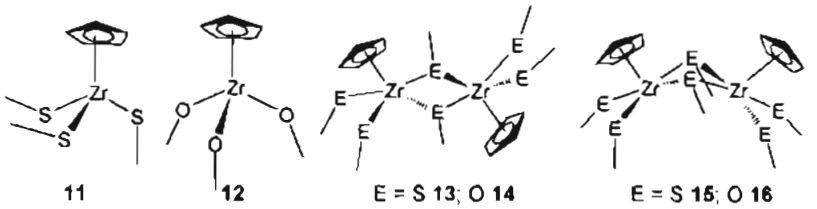

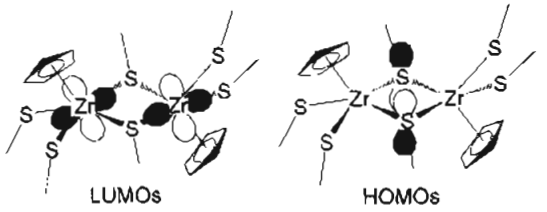

Figure 6. Schematic depiction of the two energetically degenerate HOMOs and LUMOs of the model compound $[CpZr(SMe)_2](\mu\text{-}SMe)_2$.

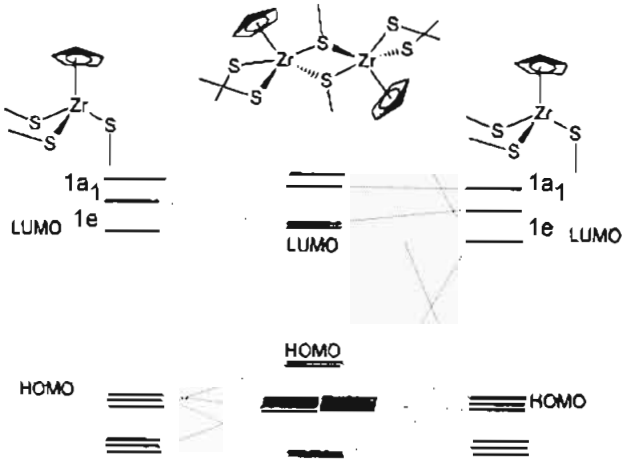

Figure 7. Molecular orbital bonding scheme for the model compound $[CpZr(SMe)_2](\mu\text{-}SMe)_2$.

ramification of the steric demands of the *cisoid* disposition of the pentamethylcyclopentadienyl rings rather than a perturbation arising from Zr−E π-bonding.

Molecular Mechanics. Models of **7** in the *cisoid* **7a** and *transoid* **7b**,**c** geometries were constructed by employing metric parameters derived from the X-ray structural data. Optimal geometries of these isomers were calculated on the basis of molecular mechanics.[17] In all cases the Zr−C and Zr−S distances and the angles in the Zr_2S_2 core were constrained to those observed crystallographically. All other parameters were variables. In the case of the *cisoid* isomer **7a**, the optimization predicts a geometry in which the bridging sulfurs are pyramidal with ethyl substituents of the bridging thiolates in a *syn* orientation. In this geometry the angle between the two ZrS_2 planes is 133°. It is noted that this orientation minimizes the transannular Cp*−Cp* interactions. As well, the *syn* orientation of the ethyl substituents on the bridging ligands precludes steric interactions between the ethyl groups and the Cp* ligands. Forced inversion of the geometry at one of the bridging S atoms results in a destabilizing interaction between the ethyl substituent and the Cp* ligands. It is this interaction that presumably inhibits inversion at S and thus the observation of only a single conformer of the *cisoid* isomer of **7**.

The *transoid* isomer of **7** can exist in two conformations, *transoid* (*anti*) **7b** and *transoid* (*syn*) **7c**. X-ray data for **7b** confirm the presence of a planar Zr_2S_2 core and pseudo-trigonal planar bridging sulfur atoms. The other conformer **7c** has been observed by NMR spectroscopy. Molecular mechanics calculations for **7c** are consistent with similar planar geometry for the bridging sulfurs and a planar Zr_2S_2 core. The interconversion of **7b** and **7c** was also considered via molecular mechanics. Calculation of the total energy as a function of rotation about the Zr−S−C−C dihedral angle was performed (Figure 8). This rotation forces the conversion between **7b** and **7c**. These data suggest a barrier between these two conformers on the order of 22.5 kcal/mol. The quantitative aspects of these calculations must be viewed with some suspicion. Nonetheless, these results are qualitatively consistent with inferences from the NMR data in that between 60 and −80 °C no evidence of interconversion of **7b** and **7c** is observed. The calculations also predict that the *transoid* (*anti*) isomer **7b** is thermodynamically more stable than the *transoid* (*syn*) isomer **7c**. Although this view may be consistent with intuitive perceptions based on symmetry, our inability to interconvert these two conformers precludes experimental confirmation of this result.

Discussion

Compounds **6** and **7** are the first examples of mono-Cp Zr thiolate derivatives. Dimerization of related Ti−thiolate systems is observed in some cases although the direct Ti analogs of **6** and **7** (i.e. $Cp^*Ti(SR)_3$) are monomeric species. The formation of the dimeric thiolate complexes **6** and **7** is consistent with both the Lewis acidity of the Zr center and the greater covalent radii and thus accessibility of Zr. The observation of only the *cisoid* isomer for **6** and a mixture of *cisoid* and *transoid* isomers for **7** suggest steric control of the dimerization process. The chemistry and bonding studies of these Cp*Zr−thiolate derivatives described above suggest the dimeric structure is quite stable. The failure of the isomers of **7** to undergo interconversion is attributable to the Lewis acidity of the Zr centers in conjunction with the basicity at sulfur. Cleavage of the dimer is a kinetically slow process that can be achieved with a strong donor (i.e. PMe_3). The complete and rapid reaction of **6** with methanol is consistent with the relative acidities of the thiol and alcohol, the oxophilicity of Zr, and the description of the HOMOs in the thiolate-bridged dimer as essentially lone pairs on the sulfur atoms.

The structural data confirm planarity at the bridging chalcogenide atoms in the *transoid* isomers of the Cp*Zr−chalcogenide dimers **7** and **9**. Molecular mechanics and EHMO calculations are consistent with the planarity at the bridging S or O atoms. This geometry places the lone pair of electrons on the bridging atoms in an orbital which is orthogonal to the vacant metal-based MOs. Thus, steric factors rather than π-bonding determine the geometry at the bridging atoms in *transoid* dimers. In a similar situation, the planar geometry at the N atom of $Cp^*_2Ti(NMePh)$[24] has been ascribed to steric factors rather than a π-interaction of the lone pair of electrons on N with Ti.

Modeling calculations also predict a pyramidal geometry for the bridging sulfur atoms in the *cisoid* isomer **7a**. This is

(24) Feldman, J.; Calabrese, J. C. *J. Chem. Soc., Chem. Commun.* **1991**, 1042.

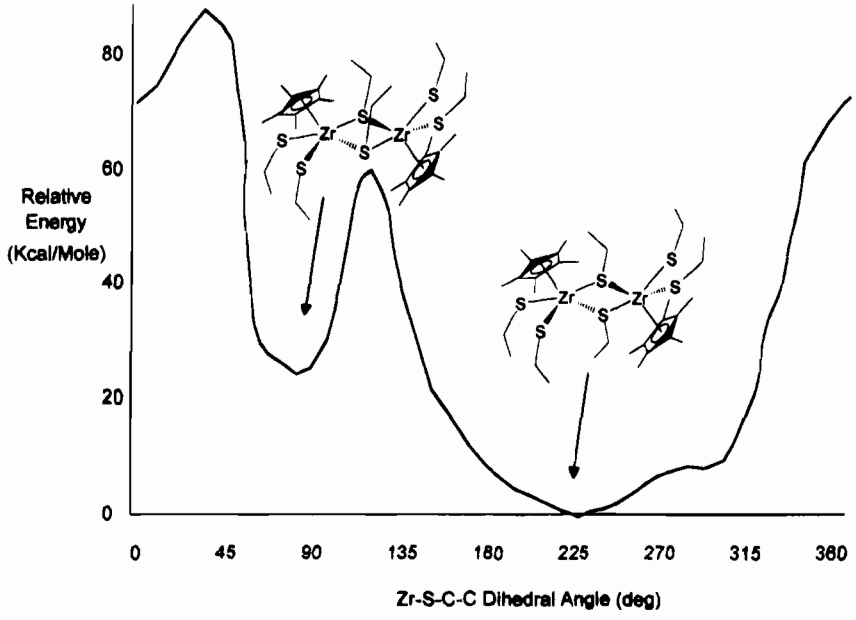

Figure 8. Plot of the total energy as calculation via molecular mechanics as a function of the Zr−S−C−C dihedral angle.

consistent with steric constraints and the absence of a π-bonding interaction between Zr and S. This view is supported to some extent by the crystallographic study of **10**. In this species, the Cp* ligands adopt a *cisoid* disposition and geometries at the bridging chalcogenide atoms (i.e. S and O) are pyramidal further suggesting that the geometry at these bridging atoms is sterically determined.

The present study is consistent with the Lewis acidity of monocyclopentadienyl complexes of Zr in general. Further investigations of related thiolate derivatives where this property can be exploited are underway.

Acknowledgment. Support from the NSERC of Canada is also acknowledged. Professor M. McGlinchey and Dr. D. Hughes (McMaster University) are thanked for helpful discussions and for the acquisition of high-field (500 MHz) NMR spectra.

Supplementary Material Available: Tables of crystallographic parameters, hydrogen atom parameters, thermal parameters, and bond distances and angles (19 pages). Ordering information is given on any current masthead page.

IC9413777